A clamp-type pressure cell for high energy x-ray diffraction

M. v. Zimmermann,[1] R. Nowak,[1] G. D. Gu,[2] C. Mennerich,[3] H.-H. Klauss,[3] and M. Hücker[2]
[1]*Hamburger Synchrotronstrahlungslabor HASYLAB at Deutsches Elektronen-Synchrotron, 22603 Hamburg, Germany*
[2]*Brookhaven National Laboratory, Upton, New York 11973, USA*
[3]*Institut für Physik der Kondensierten Materie, TU Braunschweig, 38106 Braunschweig, Germany*

(Received 9 October 2007; accepted 6 February 2008; published online 20 March 2008)

We present a clamp-type pressure cell for high energy x-ray diffraction. The pressure cell was specifically designed for studies of weak superstructure reflections at low temperatures in transition metal oxides, resulting from, e.g., charge density modulations. Using a photon energy of $E=100$ keV, the bulk properties of single crystals with a volume of typically 2–5 mm^3 can be studied in transmission geometry. To demonstrate the performance of the pressure cell, we present data on the charge stripe order in the high-temperature superconductor $La_{1.875}Ba_{0.125}CuO_4$. © *2008 American Institute of Physics.* [DOI: 10.1063/1.2889162]

I. INTRODUCTION

One avenue to uncover mechanisms behind structural and electronic ordering phenomena in correlated electron materials is to expose specimens to extreme conditions. High pressure is one of the important environments, although not always as easy to apply as temperature, magnetic or electric fields. Pressure is known to change the band structure as well as the lattice parameters, with concomitant consequences for, e.g., electronic transport, magnetism, and crystal symmetry. An excellent example for the ability of pressure to toggle between competing electronic ground states are heavy fermion systems.[1] High pressure has also been widely used in studies of high-temperature superconductors,[2–5] and diffraction experiments under pressure have provided insight into the correlation between T_c and structural parameters, such as the buckling of the CuO_2 planes and the spacing between the planes.[6–8]

A large number of different types of pressure cells have been developed for x-ray and neutron diffraction experiments, often designed for a specific purpose. In the case of x-ray diffraction, the use of diamond anvil cells (DACs) has revolutionized the field, because of attainable pressures beyond 100 GPa.[9,10] Steady progress has pushed the achievable sensitivity to about 10^{-9}.[11,12] The small dimensions of DAC are also perfectly suited for experiments at low temperatures. A disadvantage of the DAC technique can be the small sample size, typically below 100 μm in diameter and 20 μm in thickness, which makes it more sensitive to surface effects.

With large volume multianvil cells as well as the increasingly popular opposed anvil (toroid) cells of the Paris-Edinburgh-type pressures up to 30 GPa have been reached. The sample space volume can assume $\sim$100 mm^3, which is particularly useful for neutron scattering experiments, as well as techniques requiring a complex setup in the sample space.[13–15] Although single crystal diffraction is possible, in particular with toroid cells, in most cases the average crystal structure of polycrystalline materials is analyzed. Note that these devices are large and often operate at ambient or high temperatures. The Paris-Edinburgh cell, initially introduced for neutron scattering experiments at ISIS, has also been operated at low temperatures.[15] Due to the size of multianvil and toroid cells, cooling requires a liquid nitrogen or helium cryostat, and for the largest models reaching very low temperatures can be challenging.

Our goal was to design a pressure cell for the medium pressure range, that can be used with $E=100$ keV photons. Photons of this energy are extremely useful for studies of bulk properties because of their large penetration depth in solids. This is particularly important for materials which have a surface layer with a different structure.[16–18] To maximize the scattered intensity, the thickness of the sample has to be comparable to the absorption length, which can be crucial when the reflections are expected to be weak. In cuprate superconductors, such as $La_{1.875}Ba_{0.125}CuO_4$, and related transition metal oxides, the peak intensity of superstructure reflections connected to electronic order can be up to seven orders of magnitude weaker than for the strongest Bragg peak.[19] The low intensity makes single crystal diffraction mandatory, and samples with optimum thickness favorable. In the case of $La_{2-x}Ba_xCuO_4$, the absorption length at 100 keV is on the order of 1.2 mm, which is nearly two orders of magnitude larger than the typical thickness of a DAC sample. To accommodate a sample of this size, requires the use of a large volume pressure cell. A large sample space also holds the future option to insert additional experimental setups to probe other properties simultaneous with the x-ray diffraction. Another important design aspect was that the pressure cell should be lightweight, to facilitate cooling with a displex cryostat and flexible orientation in an Eulerian cradle. Based on these factors, we decided to focus on the clamp-type piston cell, which is frequently used for transport, magnetization, NMR/NQR, μSR, or optical studies.[5,13,20–22] Although maximum pressures p_{max} of 5 GPa have been achieved, typically, the upper limit for this type of

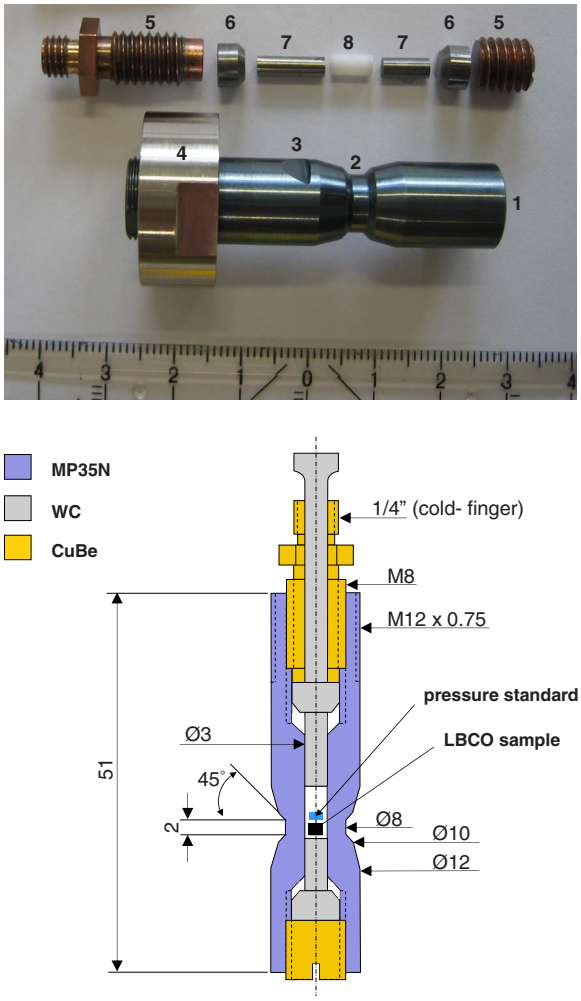

FIG. 1. (Color online) Top: pressure cell: (1) hardened MP35N pressure cell, (2) x-ray window, (3) thermometer position, (4) MP35N suspension ring, (5) hardened CuBe lock screw, (6) tungsten carbide thrust disk, (7) tungsten carbide piston, (8) Teflon sample holder. Bottom: schematic drawing of pressure cell with sample, pressure calibrant, and external piston. Dimensions in millimeter.

cell is closer to 3 GPa.[23–25] In the past, clamp cells for x-ray diffraction were equipped with Be windows to allow passage of photons with energies around 10 keV.[26] Synchrotron facilities provide sufficient flux even at x-ray energies of 100 keV, allowing photons to penetrate several millimeters of, e.g., copper. Hence, a clamp cell without beryllium or diamond window should be feasible. The setup was realized at wiggler beamline BW5 at HASYLAB, which at 100 keV ($\lambda = 0.124$ Å) provides a flux of $\sim 3 \times 10^{11}$ photons/mm^2 s on the sample.[27]

II. THE PRESSURE CELL

In Fig. 1, we show the current design of the pressure cell. The pressure chamber is made of MP35N,[25,28,29] with an inner diameter of 3 mm. All pistons and thrust disks in the figure are made of tungsten carbide, while the lock screws are made of copper-beryllium (CuBe). Thrust disks and lock screws made of MP35N have been used as well. The machined MP35N parts were heat treated at temperatures between 540 and 590 °C for 4 h and the CuBe lock screws at 325 °C for 2 h 45 min, followed by cooling at air. The total weight of the pressure cell is about 47 g. Its most characteristic feature is the x-ray window, where the outer diameter of the cell is gradually reduced from 12 to 8 mm, resulting in 2.5 mm thick walls. In this 2 mm long region, the absorption by the cell amounts 86% of the incident photon flux, only. By adjusting the bottom lock screw, the sample is brought into the center of the x-ray window. Note that, because of the high photon energy, the scattering angle 2θ rarely exceeds 7° in our experiments. Therefore, the 360° x-ray window does not have to be in the scattering plane. It can be rotated freely about the beam direction, and the beam can be tilted out of the plane of the x-ray window by 5°–10° (depends also on beam diameter) without leaving the thin walled region, which would increase the absorption. The absence of blind areas in (h,k,l) space (apart from the powder rings of MP35N), and the option to insert millimeter size spherical samples, makes this pressure cell suitable for crystallographic studies.

To increase the pressure up to which the cells can be operated, we have applied the autofrettage method.[13] For this process, the cell has an initial bore diameter of 2.5 mm. The sample space is filled with a solid Teflon cylinder. For pressurization, the cell is suspended in a ring (cf. Fig. 1) while the external piston is pushed by a hydraulic press. This way, a maximum of energy is stored after the top lock screw is tightened and the load removed, as opposed to a pressure cell that stands on its bottom side during pressurization. In the left panel of Fig. 2, we show the compression ΔL of the pressure cell versus load during the autofrettage. To be more precise, ΔL shows by how much the external piston has traveled with respect to the suspension ring (cf. Fig. 1). For loads larger than 1800 kg, the onset of a progressive compression indicates the irreversible deformation of the bore. After this procedure, the bore was honed to its final diameter of 3.0 mm.

In the right panel of Fig. 2, we show the compression ΔL versus load of the final 3 mm bore pressure cell, containing sample plus pressure calibrant in a Teflon cup, filled with DAPHNE oil as pressure transmitting medium.[30] The Teflon cups with 3 mm outer and 2.2 mm inner diameters have a length of 7–8 mm, which is sufficient to accommodate about 2.5 mm of sample and pressure calibrant without risking to crush those at high pressure. Obviously, the compressibility ΔL/load of this ensemble is smaller than during the autofrettage, mainly because the piston's cross section is larger by a factor of 1.44. For loads beyond ~2300 kg, the cell showed an enhanced compressibility, indicating that the bore started to bulge. Because of a very precise fit of pistons and bore, we have not encountered problems from leaking of Teflon or DAPHNE oil at high pressure.

The pressure cell is attached to the cold finger of a regular displex closed-cycle cryostat. The sample location is determined from the absorption profile of the pressure cell in the direct beam, measured both with and without sample. This works particularly good for samples containing high-Z elements, such as $La_{1.875}Ba_{0.125}CuO_4$. In contrast, for $CuGeO_3$, which serves us as pressure sensor (see below), the position is less obvious from the absorption profile. The ther-

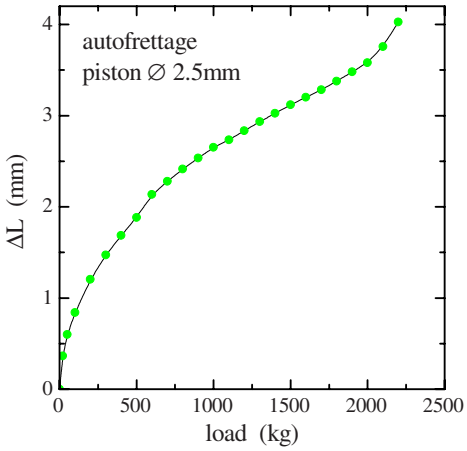

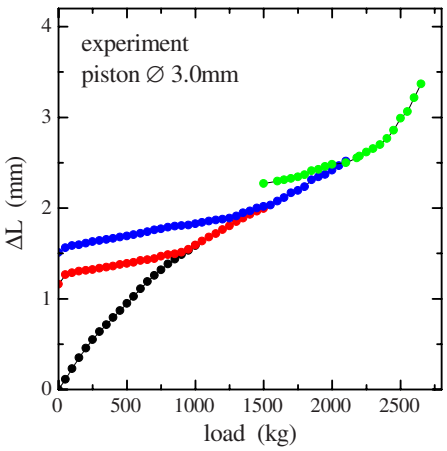

FIG. 2. (Color online) Left: compression ΔL of the pressure cell vs load during autofrettage process using a piston with 2.5 mm diameter. A Teflon cylinder served as pressure transmitting medium. Right: ΔL vs load during the experiment on a $La_{1.875}Ba_{0.125}CuO_4$ single crystal contained in a Teflon cup filled with DAPHNE oil. The Teflon cup also contained a small $CuGeO_3$ crystal. Here, a piston with 3.0 mm diameter was used.

mometer is attached from the outside on a leveled spot close to the x-ray window (cf. Fig. 1). At a cold-finger temperature of 4 K, a sample temperature of 7 K was achieved.

III. BACKGROUND SIGNAL AND PRESSURE CALIBRATION

As mentioned before, our goal is to study weak lattice modulations. Corresponding superstructure reflections can be significantly weaker than the powder lines of the MP35N cell. Therefore, one has to focus on reflections located in-between the powder lines. In Fig. 3, we show the powder spectrum of MP35N, along with the 2θ positions for some of the so-called charge stripe reflections we have been looking at in $La_{1.875}Ba_{0.125}CuO_4$. Note the logarithmic intensity scale. As shown in Fig. 8, and discussed in detail in Sec. IV, the intensity of one of the strongest charge stripe peaks is still smaller than the background signal between the powder lines. With 1/10 of the background giving about 8 counts/s at 100 mA, and with about 5×10^8 counts/s for the (1,1,0) Bragg peak, we calculate a sensitivity of $\sim2\times10^{-8}$. Although this is below the sensitivity reported for a DAC in a study on chromium in Ref. 12, it is sufficient for many problems we are facing in transition metal oxides with strongly correlated electrons.

Finally, one has to determine the pressure at low temperature. A common method is to measure the lattice parameters of a calibrant.[13] However, a characteristics of high energy beamlines, such as BW5,[27] is a particularly good transverse resolution, whereas the longitudinal resolution, needed to accurately determine lattice parameters, is only modest. Therefore, we have followed another common route, which is the determination of a pressure dependent transition. In particular, we have tracked the spin-Peierls transition temperature of $CuGeO_3$,[35] which is known to increase at a rate $dT_{SP}/dp \simeq 5$ K/GPa.[36] In Fig. 4, we plot intensity versus temperature for the (0.5, 3, 0.5) superstructure reflection,[37] which reveals a significant shift of T_{SP} to higher temperatures as the load is increased. The resulting pressures are plotted in the inset of Fig. 4. The dimensions of the $CuGeO_3$ crystal are $0.4\times1.3\times1.3$ mm^3 along the a, b, and c axes (cf. Fig. 6), and it was separated from the $La_{1.875}Ba_{0.125}CuO_4$ crystal by a 0.5 mm thick Teflon disk to avoid interfering signals.

A major problem with $CuGeO_3$ is its flaky texture. At high pressure, all reflections broadened significantly and it was increasingly difficult to determine the orientation matrix. This problem can be reduced to some extent, by covering the crystal with a thin layer of epoxy before inserting it into the

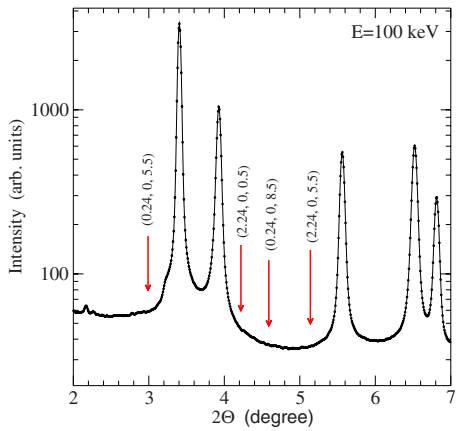

FIG. 3. (Color online) Intensity vs scattering angle for the powder spectrum of MP35N. The arrows indicate the 2θ values of a selection of superlattice reflections of interest in $La_{1.875}Ba_{0.125}CuO_4$.

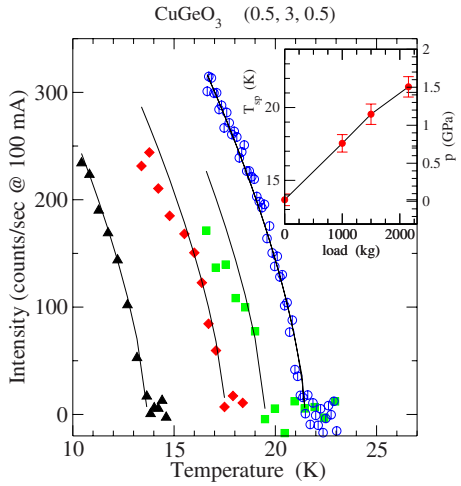

FIG. 4. (Color online) Intensity of the (0.5, 3, 0.5) superstructure reflection of $CuGeO_3$ vs temperature for different loads. The inset shows the extracted pressure values at low temperature.

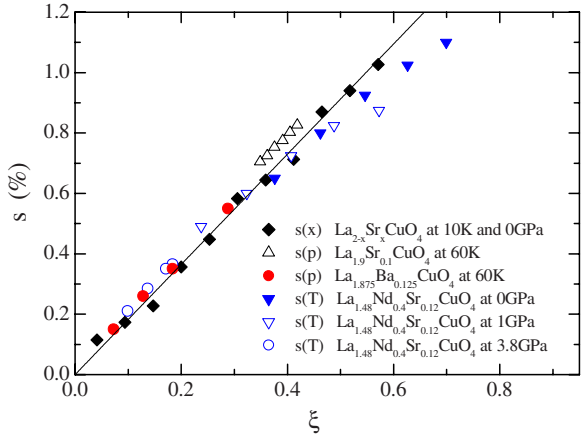

FIG. 5. (Color online) Orthorhombic strain vs parameter ξ. As described in detail in Ref. 31, $\xi=1-T^*/T_0-p/p_0-x/x_0$, where $T^*=\Theta\coth(\Theta/T)$, T_0 is the temperature of the high-temperature structural transition HTT$\leftrightarrow$LTO in La_2CuO_4 ($x=0$), and Θ accounts for the nonlinearity of $s(T)$ at low T. p_0 is the critical pressure in La_2CuO_4, and x_0 the critical Sr content in $La_{2-x}Sr_xCuO_4$ to suppress the orthorhombic phase. We have used the same parameter values (Ref. 32) as in Ref. 31, except for $La_{1.875}Ba_{0.125}CuO_4$, which has a slightly smaller x_0, and for $La_{1.48}Nd_{0.4}Sr_{0.12}CuO_4$, where we have adjusted the Sr content to $x=0.015$, to compensate the effect of Nd doping on T^* and T_0. The data for $s(x)$ in $La_{2-x}Sr_xCuO_4$ were taken from Ref. 33, $s(p)$ in $La_{1.9}Sr_{0.1}CuO_4$ from Ref. 31, $s(p)$ in $La_{1.875}Ba_{0.125}CuO_4$ this work, and $s(T)$ in $La_{1.48}Nd_{0.4}Sr_{0.12}CuO_4$ from Ref. 34.

pressure cell. However, other ways to measure the pressure were considered, and one promising method, which we plan to pursue in future experiments, is a calibration via the orthorhombic strain $s=2(a-b)/(a+b)$ in $La_{2-x}Sr_xCuO_4$ or doped analogs, where a and b are the in-plane lattice constants. In particular, when $s(p)$ is known for a certain x and T, it can be used as pressure sensor. We mention that s is an unambiguous function of x, T, and p.[31,34,38] Hence, minor changes of $s(p)$, due to variations of doping and/or T, can be corrected by using the type of scaling discussed in Ref. 31. In Fig. 5, we have reproduced some of the data shown in Ref. 31, and added our data for $La_{1.875}Ba_{0.125}CuO_4$ and data from Ref. 34 for $La_{1.48}Nd_{0.4}Sr_{0.12}CuO_4$, showing that s scales approximately linear with T, p, and x, as is explained in the figure caption. We mention that the range and accuracy of the scaling can be improved by taking non-linear effects into account. The purpose of this discussion is to point out that there is no need to perform a full calibration each time a different piece of crystal is used as pressure sensor, as long as chemical compositions are not too different. It is natural that specimens from different batches will have slightly different properties. These differences, however, can be scaled. Moreover, crystals grown by the traveling-solvent floating-zone method typically measure several centimeters in length and 5–8 mm in diameter, which provides enough material for a large number of pressure probes from the same batch. Another clear advantage of this method is that, at low temperatures, s changes only slowly as a function of T. Thus, for $p(s)$, temperature is not as critical as it is for methods that depend on a precisely measured structural or superconducting transition temperature.

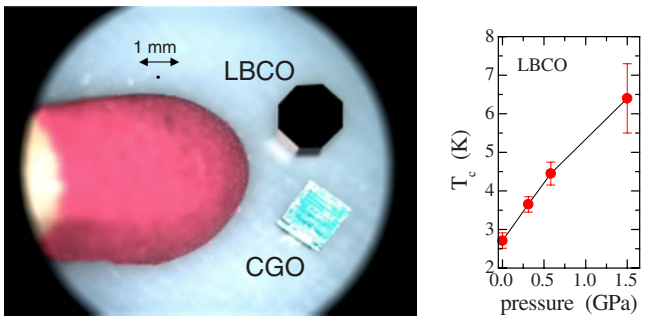

FIG. 6. (Color online) Left: single crystals of $La_{1.875}Ba_{0.125}CuO_4$ (black) and $CuGeO_3$ (blue). $CuGeO_3$ is used as a pressure calibrant. The red object is a match head (for scale). The black dot below the scale indicates the typical size of a sample that fits into a DAC. Right: pressure dependence of T_c in $La_{1.875}Ba_{0.125}CuO_4$ as determined from ac susceptibility in magnetic fields between 0.1 and 3 Oe (Ref. 39).

IV. SCIENCE EXAMPLE: CHARGE STRIPE ORDER IN LBCO

The design of the pressure cell was tailored to meet the requirements set by the weak intensity of the charge stripe reflections in $La_{2-x}Ba_xCuO_4$.[19] This high-temperature superconductor[40] is known to display an intriguing interplay between structural and electronic properties.[41–43] In particular, at a Ba content of $x=1/8$, superconductivity is strongly affected by the appearance of a competing ground state also known as the stripe phase.[44] In this phase, the charge carriers segregate into one-dimensional hole-rich stripes, which form the boundaries between intermediate regions of antiferromagnetic spin stripes with low charge carrier concentration.[44,45] At ambient pressure, the appearance of the stripe phase is triggered by a particular structural transformation, which can be influenced with pressure.[34] Pressure also leads to an increase of the superconductivity, as can be seen from our data for $T_c(p)$ in Fig. 6, obtained by susceptibility measurements.[39] However, the effect of pressure on the stripe order is not known.

For the experiment, we have used a $La_{1.875}Ba_{0.125}CuO_4$ single crystal grown by the traveling-solvent floating-zone method. To optimize the signal to background ratio, it was polished into the shape of an octagonal prism 1.6 mm in diameter and 1.3 mm in height (cf. Fig. 6). This leaves some space between the sample and the wall of the Teflon cup which may help to maintain hydrostatic conditions as good as possible. The incident beam size was set to 1×1 mm^2, i.e., slightly smaller than the sample. At ambient pressure, $La_{1.875}Ba_{0.125}CuO_4$ shows two structural transitions: from the high-temperature-tetragonal (HTT) phase to the low-temperature-orthorhombic (LTO) phase at $T_{HT}\simeq235$ K, and from the LTO phase to the low-temperature-tetragonal (LTT) phase at $T_{LT}\simeq54$ K. We refer to Ref. 42 for details of the crystal structure. In the following, all structural phases are indexed on the basis of the HTT phase with space group $I4/mmm$ and lattice parameters $a=b=3.78$ Å and $c=13.2$ Å. In the orthorhombic phase, $La_{1.875}Ba_{0.125}CuO_4$ forms twin domains, which makes it easy to determine the orthorhombic strain by means of transverse scans through the pair of $(2,0,0)/(0,2,0)$ Bragg reflections. Figure 7 pre-

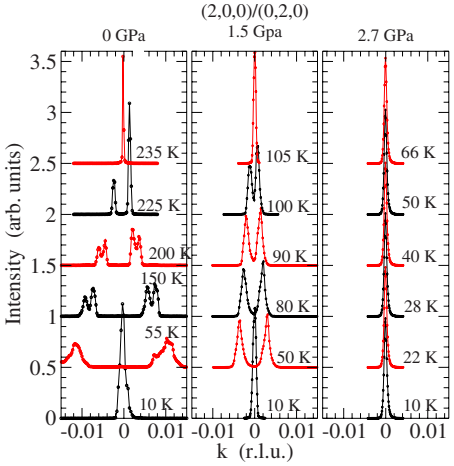

FIG. 7. (Color online) Orthorhombic strain at $p=0$, 1.5, and 2.7 GPa for various temperatures, as determined from transverse scans through the $(2,0,0)/(0,2,0)$ Bragg peaks. The additional split of the reflections in the orthorhombic phase at $p=0$ and 55 K$\leqslant T\leqslant$150 K most likely indicates a weak monoclinic distortion, previously observed in La_2CuO_4 (Ref. 46).

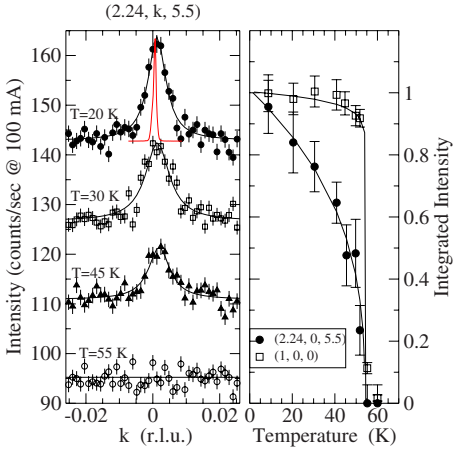

FIG. 8. (Color online) Left: k scans through the charge stripe order peak at $\mathbf{Q}=(2.24,0,5.5)$ of the $La_{1.875}Ba_{0.125}CuO_4$ crystal (mounted in the pressure cell) at different temperatures. These data are for ambient pressure. All scans, except the one at $T=55$ K, are shifted for clarity. A corresponding scan through the nearby (2, 0, 6) Bragg reflection at 20 K indicates the instrumental resolution (solid red line). The background signal of the pressure cell is 80 counts/s, the sample contributes another 15 counts/s to the background. At $T=20$ K, the ratio between peak intensity and combined background is about 1:5. Right: normalized integrated intensity of the (2.24, 0, 5.5) charge peak and the (1, 0, 0) LTT peak vs temperature.

sents corresponding scans at various temperatures for $p=0$, 1.5, and 2.7 GPa. The results for $p=2.7$ GPa were obtained with a slightly modified cell, as is explained further below. One can clearly see the effect of pressure, which suppresses the HTT$\leftrightarrow$LTO transition. For $p=0$ and 1.5 GPa, the single Bragg reflection at 10 K indicates that the sample is in the LTT phase. For $p=2.7$ GPa, the sample is in the HTT phase at all temperatures. Note the high transverse resolution, which allows a precise measurement of s. See Refs. 34 and 47 for corresponding results from x-ray powder diffraction and single crystal neutron diffraction on similar materials.

The charge stripe order is observed in the LTT phase, where it leads to additional reflections with ordering wave vector $\mathbf{g}_{CO}=(0.24,0,0.5)$.[44,48] We have studied a relatively strong reflection with scattering vector $\mathbf{Q}=(2.24,0,5.5)$ and low MP35N background signal (cf. Fig. 3). In Fig. 8, we show scans along $\mathbf{Q}=(2.24,k,5.5)$ for different temperatures at ambient pressure. Count time is 40 s/point. Apparently, the intensity of the (2.24,0,5.5) charge peak decreases with increasing temperature and vanishes right at the LTT$\leftrightarrow$LTO transition, marked by the disappearance of the (1, 0, 0) superstructure peak. This data set clearly demonstrates that, with the new pressure cell, it is possible to study the charge stripe order in $La_{1.875}Ba_{0.125}CuO_4$ under pressure, using a bulk sensitive transmission geometry. Corresponding x-ray results, along with a detailed study of the superconducting properties, will be published elsewhere.[39]

We mention that, in a recent experiment, we have reached $p=2.7(3)$ GPa using a slightly modified cell with a 2.5 mm bore and a x-ray window with an outer diameter of 8.7 mm. This pressure was sufficient to suppress the orthorhombic phase, as is shown in Fig. 7. No autofrettage was performed on this cell. A load of 2200 kg was applied without significant deformation of the bore. In this run, no $CuGeO_3$ pressure standard was inserted, so that a rough estimate of p was extracted from the pressure dependence of the c-axis lattice parameter of $La_{2-x}Ba_xCuO_4$. A fit to the 2θ values of the (002), (004), (006), and (008) Bragg reflections resulted in $c=13.115$ Å, compared to $c=13.2$ Å at ambient pressure. Using a typical value of $\kappa_c=2.4(4)\times10^{-3}$/GPa for the compressibility of the c axis of tetragonal $La_{2-x}Sr_xCuO_4$ near optimum doping, the above mentioned value of 2.7 GPa was determined.[31,49,50] The sensitivity of this cell is approximately 38% lower, but still sufficient to detect the charge stripe reflections.

V. CONCLUSION

To summarize, we have designed a clamp-type pressure cell suited for hard (100 keV) x-ray diffraction applications. The structure of single crystals with a volume of several cubic millimeters can be studied in the bulk sensitive transmission geometry up to pressures of ~2.7 GPa at low temperatures. With some improvements, a pressure of 3.5 GPa should be feasible. These improvements include optimization of the autofrettage process and the heat treatment of MP35N, as well as the modification of certain dimensions, such as the heights and thickness of the x-ray window. The current design of the 360° x-ray window, together with the small scattering angles for 100 keV photons, provides easy access to a wide region of the reciprocal space. Low weight and small dimensions of the pressure cell allow cooling with a displex cold finger. The large sample space will enable us to insert additional experimental setups for simultaneous probing of other properties during the x-ray experiment. The pressure cell is particularly useful for bulk studies of extremely weak reflections, such as those resulting from charge density modulations in correlated electron systems.

ACKNOWLEDGMENTS

We would like to thank J. S. Schilling and M. Debessai for discussions and for providing the pressure dependence of T_c in $La_{2-x}Ba_xCuO_4$. M.H. is grateful for discussions with

J. M. Tranquada. We also would like to thank U. Maul for machining the pressure cells. The $CuGeO_3$ crystal was grown by I. Tsukada and K. Uchinokura. The work at Brookhaven was supported by the Office of Science, U.S. Department of Energy under Contract No. DE-AC02-98CH10886.

[1] N. D. Mathur, F. M. Grosche, S. R. Julian, I. R. Walker, D. M. Freye, R. K. W. Haselwimmer, and G. G. Lonzarich, Nature (London) **394**, 39 (1998).
[2] L. Gao, Y. Y. Xue, F. Chen, Q. Xiong, R. L. Meng, D. Ramirez, and C. W. Chu, Phys. Rev. B **50**, 4260 (1994).
[3] W. J. Liverman, J. G. Huber, A. R. Moodenbaugh, and Y. Xu, Phys. Rev. B **45**, 4897 (1992).
[4] K. Yamada, K. Kakurai, Y. Endoh, T. R. Thurston, M. A. Kastner, R. J. Birgeneau, G. Shirane, Y. Hidaka, and T. Murakami, Phys. Rev. B **40**, 4557 (1989).
[5] J. S. Schilling, in *Handbook of High-Temperature Superconductivity: Theory and Experiment*, edited by J. R. Schrieffer (Springer, Hamburg, 2007), p. 427.
[6] N. Yamada and M. Ido, Physica C **203**, 240 (1992).
[7] M. Ido, N. Yamada, and M. Oda, Physica B **194–196**, 2069 (1994).
[8] O. Chmaissem, J. D. Jorgensen, S. Short, A. Knizhnik, Y. Eckstein, and H. Shaked, Nature (London) **397**, 45 (1999).
[9] A. Jayaraman, Rev. Mod. Phys. **55**, 65 (1983).
[10] R. Letoullec, J. P. Pinceaux, and P. Loubeyre, High Press. Res. **1**, 77 (1988).
[11] Y. Feng, M. S. Somayazulu, R. Jaramillo, T. F. Rosenbaum, E. D. Isaacs, J. Hu, and H. K. Mao, Rev. Sci. Instrum. **76**, 063913 (2005).
[12] Y. Feng, R. Jaramillo, G. Srajer, J. C. Lang, Z. Islam, M. S. Somayazulu, O. G. Shpyrko, J. J. Pluth, H. K. Mao, E. D. Isaacs, G. Aeppli, and T. F. Rosenbaum, Phys. Rev. Lett. **99**, 137201 (2007).
[13] M. I. Eremets, *High Pressure Experimental Methods* (Oxford University, New York, 1996).
[14] J. M. Besson, G. Weill, G. Hamel, R. J. Nelmes, J. S. Loveday, and S. Hull, Phys. Rev. B **45**, 2613 (1992).
[15] S. Klotz, J. M. Besson, G. Hamel, R. J. Nelmes, J. S. Loveday, W. G. Marshall, and R. M. Wilson, Appl. Phys. Lett. **66**, 1735 (1995).
[16] K. H. Conlon, H. Luo, D. Viehland, J. F. Li, T. Whan, J. H. Fox, C. Stock, and G. Shirane, Phys. Rev. B **70**, 172204 (2004).
[17] G. Xu, P. M. Gehring, C. Stock, and K. H. Conlon, Phase Transitions **79**, 135 (2006).
[18] H. Hünnefeld, T. Niemöller, J. R. Schneider, U. Rütt, S. Rodewald, J. Fleig, and G. Shirane, Phys. Rev. B **66**, 014113 (2002).
[19] H. Kimura, H. Goka, M. Fujita, Y. Noda, K. Yamada, and N. Ikeda, Phys. Rev. B **67**, 140503 (2003).
[20] B. Simovič, M. Nicklas, P. C. Hammel, M. Hücker, B. Büchner, and J. D. Thompson, Europhys. Lett. **66**, 722 (2004).
[21] H.-H. Klauss, D. Baabe, D. Mienert, H. Luetkens, F. J. Litterst, B. Büchner, M. Hücker, D. Andreica, U. Zimmermann, and A. Amato, Physica B **312**, 71 (2002).
[22] K. H. Satoha, T. Gokoa, S. Takeshitaa, Y. Hayashia, J. Araia, W. Higemotob, K. Nishiyamac, and K. Nagaminec, Physica C **374**, 40 (2006).
[23] A. Lavergne and E. Whalley, Rev. Sci. Instrum. **49**, 923 (1978).
[24] D. B. McWhan, D. Bloch, and G. Parisot, Rev. Sci. Instrum. **45**, 643 (1974).
[25] I. R. Walker, Rev. Sci. Instrum. **70**, 3402 (1999).
[26] K. Pressl, M. Kriechbaum, M. Steinhart, and P. Laggner, Rev. Sci. Instrum. **68**, 4588 (1997).
[27] R. Bouchard, D. Hupfeld, T. Lippmann, J. Neuefeind, H.-B. Neumann, H. F. Poulsen, U. Rütt, T. Schmidt, J. R. Schneider, J. Süssenbach, and M. von Zimmermann, J. Synchrotron Radiat. **5**, 90 (1998).
[28] K. Han, A. Ishmaku, Y. Xin, H. Garmestani, V. J. Toplosky, R. Walsh, C. Swenson, B. Lesch, H. Ledbetter, S. Kim, M. Hundley, and J. R. Sims, Jr., IEEE Trans. Appl. Supercond. **12**, 1244 (2002).
[29] D. Mienert, Ph.D. thesis, Technische Universität Braunschweig, 2006.
[30] Produced by Idemitsu Co., Ltd. Tokyo, Japan.
[31] H. Takahashi, H. Shaked, B. A. Hunter, P. G. Radaelli, R. L. Hitterman, D. G. Hinks, and J. D. Jorgensen, Phys. Rev. B **50**, 3221 (1994).
[32] In Ref. 31, the following values were reported: T_0=557 K, Θ=62 K, p_0=7.2 GPa, and x_0=0.236. These values have to be refined when nonlinear effects are included.
[33] P. G. Radaelli, J. D. Jorgensen, R. Kleb, B. A. Hunter, F. C. Chou, and D. C. Johnston, Phys. Rev. B **49**, 6239 (1994).
[34] M. K. Crawford, R. L. Harlow, S. Deemyad, V. Tissen, J. S. Schilling, E. M. McCarron, S. W. Tozerm, D. E. Cox, N. Ichikawa, S. Uchida, and Q. Huang, Phys. Rev. B **71**, 104513 (2005).
[35] M. Hase, I. Terasaki, and K. Uchinokura, Phys. Rev. Lett. **70**, 3651 (1993).
[36] H. Takahashi, N. Mori, O. Fujita, J. Akimitsu, and T. Matsumoto, Solid State Commun. **52**, 817 (1995).
[37] K. Hirota, D. E. Cox, J. E. Lorenzo, G. Shirane, J. M. Tranquada, M. Hase, K. Uchinokura, H. Kojima, Y. Shibuya, and I. Tanaka, Phys. Rev. Lett. **73**, 736 (1994).
[38] P. G. Radaelli, D. G. Hinks, A. W. Mitchell, B. A. Hunter, J. L. Wagner, B. Dabrowski, K. G. Vandervoort, H. K. Viswanathan, and J. D. Jorgensen, Phys. Rev. B **49**, 4163 (1994).
[39] M. Hücker, M. v. Zimmermann, M. Debessai, J. S. Schilling, G. Gu *et al.* (unpublished).
[40] J. G. Bednorz and K. A. Müller, Z. Phys. B: Condens. Matter **64**, 189 (1986).
[41] A. R. Moodenbaugh, Y. Xu, M. Suenaga, T. J. Folkerts, and R. N. Shelton, Phys. Rev. B **38**, 4596 (1988).
[42] J. D. Axe, A. H. Moudden, D. Hohlwein, D. E. Cox, K. M. Mohanty, A. R. Moodenbaugh, and Y. Xu, Phys. Rev. Lett. **62**, 2751 (1989).
[43] N. Yamada, M. Oda, M. Ido, Y. Okajima, and K. Yamaya, Solid State Commun. **70**, 1151 (1989).
[44] M. Fujita, H. Goka, K. Yamada, J. M. Tranquada, and L. P. Regnault, Phys. Rev. B **70**, 104517 (2004).
[45] J. M. Tranquada, B. J. Sternlieb, J. D. Axe, Y. Nakamura, and S. Uchida, Nature (London) **375**, 561 (1995).
[46] M. Reehuis, C. Ulrich, K. Prokeš, A. Gozar, G. Blumberg, S. Komiya, Y. Ando, P. Pattison, and B. Keimer, Phys. Rev. B **73**, 144513 (2006).
[47] M. Fujita, H. Goka, K. Yamada, and M. Matsuda, Phys. Rev. B **66**, 184503 (2002).
[48] M. von Zimmermann, A. Vigliante, T. Niemöller, N. Ichikawa, T. Frello, J. Madsen, P. Wochner, S. Uchida, N. H. Andersen, J. M. Tranquada, D. Gibbs, and J. R. Schneider, Europhys. Lett. **41**, 629 (1998).
[49] H. Takahashi, C. Murayama, S. Yomo, N. Mori, K. Kishio, K. Kitazawa, and K. Fueki, Jpn. J. Appl. Phys., Part 2 **26**, L504 (1987).
[50] G. Oomi, T. Kagayama, and T. Takemura, Physica C **185**, 889 (1991).